55th International Conference on Environmental Systems
12-16 July 2026, Rio Grande, Puerto Rico ICES-2026-164

Artemis Suit Material Optical Property Testing of Dust Exposed Fabrics

Robert J. Jones[1]
Leidos / KBR HHPC / NASA Johnson Space Center, Houston, TX, 77058

Shane McFarland[2]
Aegis Aerospace / KBR HHPC / NASA Johnson Space Center, Houston, TX 77058

Stephanie Rodgers-Ahnen[3]
Textile Made, Inc., Howell, MI 48843

Colton Peabody[4]
Barrios / Amentum Technology / NASA Johnson Space Center, Houston, TX, 77058

and

Felix Arwen[5]
Nexus Solutions / Amentum Technology / NASA Johnson Space Center, Houston, TX, 77058

This paper highlights one aspect of NASA's ongoing technology-infusion effort to design, fabricate, and test a next-generation outer shell fabric for a lunar Extravehicular Activity (EVA) space suit, a critical component of sustained lunar exploration. Managing thermal loads on the Moon is essential for astronaut safety and suit performance. The suit's exterior fabric directly influences heat gain and loss through its optical properties: low solar absorptivity minimizes sunlight absorption, while high infrared emissivity aids radiative cooling. Lunar regolith complicates this balance. Its fine, abrasive particles possess unique optical behavior that can lower reflectivity and raise emissivity when embedded in or adhered to fabric surfaces, degrading thermal control and increasing the risk of overheating or cooling inefficiency. To quantify these effects, the Artemis Suit Materials (ASM) team measured solar absorptance and infrared emissivity of clean and dust-soiled Ortho Fabric, establishing beginning-of-life (BOL) and end-of-life (EOL) benchmarks. EOL conditions were simulated with a rotary tumbler abrasion process using lunar dust simulant and ceramic media to reproduce cumulative wear expected during surface operations. Tests also included unmodified fabrics and a fabric/film laminate system containing titanium dioxide to evaluate potential improvements in dust resistance and optical performance. Results from these evaluations provide critical insight into how lunar dust alters fabric thermal behavior and inform the design of bespoke suit materials that maintain required optical properties throughout mission life, supporting safe and effective long-duration EVA on the lunar surface.

[1] Space Suit Engineer, Crew and Thermal Systems Division, NASA Johnson Space Center, Houston, TX.
[2] Technology and Development Lead, Crew and Thermal Systems Division, NASA Johnson Space Center, Houston, TX.
[3] Textile Engineer, Textile Made, Howell, MI.
[4] Space Suit Test Engineer, Crew and Thermal Systems Division, NASA Johnson Space Center, Houston, TX.
[5] Lead Space Suit Fabricator, Crew and Thermal Systems Division, NASA Johnson Space Center, Houston, TX.

Acronyms and Nomenclature

AML	=	Advanced Materials Laboratory
AO	=	Atomic Oxygen
ASM	=	Artemis Suit Materials
ASTM	=	American Society for Testing and Materials
BOL	=	Beginning of Life
EOL	=	End of Life
EPG	=	Environmental Protection Garment
EVA	=	Extravehicular Activity
ePTFE	=	Expanded Polytetrafluoroethylene
IR	=	Infrared
LEO	=	Low Earth Orbit
LPSR	=	Laboratory Portable Spectro Reflectometer
MISSE	=	Materials Internation Space Station Experiment
MLI	=	Multi-Layer Insulation
Nm	=	Nano Meter
PSR	=	Permanently Shadowed Region
PTFE	=	Polytetrafluoroethylene
RPM	=	Rotations per minute
SBIR	=	Small Business Innovation Research
TiO_2	=	Titanium Dioxide
UV	=	Ultraviolet

I. Introduction

IN the harsh environment of the Moon, managing heat is critical for astronaut safety and suit performance. The suit's exterior fabric plays a key role in the way it interacts with energy from the sun due to its optical properties. Lighter colors, like white, reflect more sunlight, reducing solar absorption, while materials with high infrared emissivity help dissipate heat, maintaining thermal equilibrium. Solar absorptivity refers to how much sunlight a material absorbs, whereas infrared emissivity is the ability of a material to release absorbed heat as infrared radiation. For a space suit, these properties must be carefully controlled to avoid overheating. This balance is essential for ensuring the suit's functionality and protecting astronauts from extreme temperature swings on the Moon.

Lunar regolith has unique optical properties due to its composition, particle size distribution, and high surface area. It reflects and emits radiation differently than clean fabric surfaces, with a tendency to lower reflectivity and increase thermal emissivity, especially in the infrared spectrum[1]. When lunar dust becomes embedded in or adheres to the surface of a space suit fabric, it can significantly alter the fabric's original optical behavior. The extent of this alteration depends on both the amount of regolith retained and how deeply it is embedded in the weave or coating. As a result, soiling by lunar dust may degrade a fabric's ability to reflect solar radiation or manage thermal load, impacting thermal control performance and potentially increasing the risk of overheating or cooling inefficiencies during extravehicular activities (EVAs). Quantifying and understanding these effects are critical for designing a bespoke fabric for optimal suit performance in the lunar environment.

Therefore, the Artemis Suit Materials (ASM) team conducted absorptance and emissivity testing on fabrics to determine if they meet the current optical property requirements, set by measuring the "baseline" values of both clean and dirty (soiled by lunar simulant) Ortho Fabric. The team aimed to assess fabric performance in both the beginning-of-life (BOL) condition and the more degraded end-of-life (EOL) state. To simulate the EOL condition, fabric samples were exposed to a rotary tumbler abrasion stressor which uses lunar dust simulant and ceramic tumbler media to create cumulative mechanical wear expected during lunar surface operations. This process is further detailed in Section II, C. Several commercial fabrics were included in the test as well as a fabric/film laminate system which incorporated titanium dioxide (TiO_2). The team wanted to explore the effects that the additive and films would have on the fabric's ability to resist dust and improve optical properties.

Fabric optical property requirements for the ASM project are listed in Table 1 for reference, and the full ASM fabric requirements are detailed in ICES-2026-56.

Table 1: ASM Fabric Optical Property Requirements

	ASTM	Threshold Clean (BOL)	Threshold Dirty (EOL)	Goal
Absorptance	C1549	<0.3	<0.6	<0.2
Emissivity	E408	>0.8		>0.9

II. Testing Background

A. ASTM C1549 Absorptance

Solar absorptance properties for candidate Environmental Protection Garment (EPG) fabrics were measured by the ASM Team in accordance with ASTM C1549, "Standard Test Method for Determination of Solar Reflectance Near Ambient Temperature Using a Portable Solar Reflectometer[2]." This method was selected based on the availability and suitability of the Devices & Services 410 Solar Reflectometer device, which enables rapid, repeatable measurement of broadband solar reflectance across a large population of candidate materials. The approach aligned with ASM trade-study objectives to compare optical performance across fabric constructions, finishes, and exposure conditions in a timely manner.

It is noted that ASTM C1549 differs from laboratory-based methods such as ASTM E903, "Standard Test Method for Solar Absorptance, Reflectance, and Transmittance of Materials Using Integrating Spheres[3]", in both measurement approach and intent. ASTM E903 employs a spectrophotometer with an integrating sphere to measure spectral reflectance and transmittance across the solar spectrum, enabling direct calculation of absolute solar absorptance with high accuracy. While E903 provides greater fidelity and the ability to independently resolve reflectance, absorptance, and transmittance, it requires specialized laboratory equipment, larger and more idealized specimens, and significantly longer test times. In contrast, ASTM C1549 uses a portable, filtered-detector reflectometer calibrated to approximate broadband solar reflectance, allowing efficient screening and comparative evaluation without full spectral resolution[4].

One caveat is that ASTM C1549 is written for optically opaque materials and therefore does not address or prescribe the use of different backing materials during testing. The method assumes that solar transmittance is negligible and that absorptance may be inferred directly as one minus reflectance. ASTM E903 explicitly requires different backing materials which enables the separation of reflectance, absorptance, and transmittance. In this effort, the ASM team elected to selectively use backing materials to explore the effect of the real-world reflective behavior of the EPG system and to enable comparative evaluation of partially translucent fabrics. This approach is consistent with the physical principles described in ASTM E903 but is not explicitly defined within ASTM C1549.

The following definitions and calculations establish the framework for the calculated test results presented in Section III. They are defined in ASTM E903. Absorptance (α) is defined as the fraction of incident solar energy absorbed by a material, reflectance (ρ) is the fraction reflected back into space, and transmittance (τ) is the fraction transmitted through the material when it is not optically opaque.

For opaque materials, solar absorptance may be inferred directly as:

$$\propto = 1 - reflectance\ (\rho)$$

However, for non-opaque materials—such as thin polymers, light-colored or porous textiles, or coated fabrics with partial transparency—solar transmittance must also be considered. Transmittance is defined as:

$$\tau = \frac{Transmitted\ Energy}{Incident\ Energy}$$

As mentioned, to isolate absorptance from transmittance in such cases ASTM E903 prescribes the use of different backing materials placed behind the specimen during measurement. A black backing, which has high absorptance ($\alpha \approx 1$), absorbs nearly all transmitted radiation and is used to simulate a worst-case heat absorption scenario. A reflectance measurement taken with a black backing (Rb) yields the total apparent absorptance:

$$\propto_{total} = 1 - R_b$$

A highly reflective mirror backing ($\rho \approx 1$) is also used to reflect nearly all transmitted radiation back through the sample. A reflectance measurement taken with the mirror backing (Rm) minimizes the influence of transmission and helps isolate the front-surface optical behavior of the material. The transmitted component may then be estimated by subtracting the two measurements:

$$T = R_m - R_b$$

In real-world applications, the amount of solar radiation transmitted through the outer shell fabric depends on what lies beneath it in the EPG layup. For the Artemis suit architecture, the backing layer is aluminized Mylar insulation, also referred to as multilayer insulation (MLI), which has a highly reflective, mirror-like surface. To more accurately simulate these operational conditions during testing, aluminized Mylar was used in place of an idealized mirror backing to represent the reflective behavior of the full fabric system.

Accordingly, consistent with the methodology defined in NASA report NASA/TP-2019-220552 “Calculated Transmission Using a Portable Spectroreflectometer”[5] and illustrated in Figure 1, three measurements are collected to

$$\tau = \frac{1}{2}\left[-\rho_{\text{sample}} + \sqrt{\frac{4x - 4\rho_{\text{sample}} + \rho_{\text{mirror}}\rho^{2}_{\text{sample}}}{\rho_{\text{mirror}}}}\right]$$

Calculate the solar absorptance, α_s:

$$\alpha_s = 1 - \rho_{\text{sample}} - \tau_s$$

where

τ = transmission
ρ_{sample} = reflectance of sample measured with blackbody backing
x = reflectance of sample measured with reflective backing
ρ_{mirror} = reflectance of reflective backing.

Figure 1. Solar Transmittance (τ) and Solar Absorbance (α) Formula. *To calculate the transmissivity of the fabric, three measurements are taken and used in this equation.*

determine solar transmittance and absorptance for partially translucent fabrics: (1) the reflectance of the sample with a black backing, (2) the reflectance of the sample with a reflective backing (MLI), and (3) the reflectance of the reflective backing (MLI) alone.

The solar transmittance is then subtracted from the as-measured solar absorptance obtained with the black backing to estimate the effective absorptance of the fabric within the representative EPG system configuration.

It is noted that absorptance and absorptivity are related but distinct concepts used to describe interactions between materials and electromagnetic radiation. Absorptance refers to the measured fraction of incident radiation absorbed under specific test conditions and is the appropriate term for reporting laboratory measurements. Absorptivity, by contrast, is an idealized material property defined at a specific wavelength and temperature and is typically used in theoretical analyses or modeling[6]. As such, absorptance is used throughout this report when presenting experimental results.

B. ASTM E408 Emissivity

Emissivity measurements were made by following ASTM E408 “Standard for Test Methods for Total Normal Emittance of Surfaces Using an Emissometer.[7]” It describes a method for measuring the total hemispherical emissivity (simplified as “emittance”) of materials. Emittance is the efficiency with which a surface radiates thermal energy compared to a blackbody (ε=1).

Similar to absorptivity, the backer material can affect the emissivity measurement if the specimen is semi-transparent to thermal infrared radiation. If the specimen is semi-transparent or thin, a black backer may lead to higher measured emissivity due to its strong IR emission. An MLI backer reflects internal radiation and may lower measured emissivity. A black backer will provide a conservative estimate (worst-case heating) while an MLI backer will simulate more real-world conditions because it mimics suit layup construction.

C. Fabric Conditioning

To create simulant laden fabric, each was subjected to the ASM rotary tumbler abrasion test[8]. The rotary tumbler configuration, as shown in Figure 2, is comprised of six 13” x 8” gasketed clamping frames fastened to the sides of a hexagonal drum. One panel of each fabric type was labeled, weighed, photographed, and then captured under a frame along with clear polycarbonate plastic sheet of the same size. The four fabrics were mounted so that their face side was to the interior of the drum. The fabrics were clamped around their edges but not tensioned, allowing them to deflect when impacted based on the stretch of the material. Two slots on the tumbler were left empty with only the clear plastic sheet and frame mounted to seal the openings. Before the final panel was mounted, 453.5g (1 lb.) of lunar simulant and 453.5g (1 lb.) of ceramic tumbler media rocks were added to the interior of the drum, as shown in Figure 2.

Figure 2. Rotary Abrasion Tumbler. *(Left)Exterior of tumbler drum and roller base. (Right top) Interior of drum showing lunar dust simulant and ceramic media. (Right bottom) A full panel of dust covered Ortho Fabric.*

The rotary drum was placed on a powered roller base which provided an eight-hour tumble duration at a roller spin speed of 80 rpm. The drum was flipped halfway through the duration to ensure that the abradant was equally distributed in case of biasing to one end of the drum. Once completed, the drum was removed from the roller base and the frames were removed. Any simulant that penetrated through a fabric panel was captured between the backside of the fabric and the sheet of plastic. Upon removal of the fabric panel, the penetrated dust simulant was collected and weighed. The fabric panels were cleaned per a prescribed method (brushing and vacuuming in a consistent manner), weighed, photographed, and prepared for testing. Further definition of the tumbler exposure is found in ICES-2023-37[9] and ICES-2024-50[10].

Typically, NU-LHT-4M dust simulant is used exclusively by the ASM team in the rotary tumbler tests. However, for this evaluation, the team chose to run a single fabric, Ortho Fabric, with an alternate simulant, CSM-LHT-1, to assess how the choice of simulant may influence changes in optical properties. This comparison was intended to determine whether different simulant compositions and particle characteristics produce measurable differences in fabric optical property degradation.

After the fabrics were conditioned in the rotary tumbler test and cleaned, absorptance and emissivity measurements were taken of both the BOL and EOL versions for comparison.

D. Fabrics Included in Evaluation

The fabrics that were tested and measured by the ASM team are detailed in Table 2.

Table 2: Fabric Description and Simulant Type Used

Fabric Name	Part Number	Manufacturer	Fiber Type	Simulant Type	Penetrated (g)
Ortho Fabric	116	FDI	Gore-Tex, Nomex, Kevlar	NU-LHT-4M CSM-LHT-1	5.04 4.58
Teflon™	T-162	Stern & Stern	PTFE	NU-LHT-4M	5.86
JPS Kevlar®	775 KM2 Plus	Dunmore/Dupont	Kevlar	NU-LHT-4M	0.58
PTFE Laminated Kevlar®	400-00129-03	Force Engineering	Kevlar	NU-LHT-4M	0.00

These four fabrics were included in the optical properties testing to aid in establishing performance baselines and explore potential material improvements. Ortho Fabric and Teflon™ T-162 are considered heritage materials as both are used on the existing Extravehicular Mobility Unit (EMU) suit. JPS Kevlar® was selected as a fabric of interest due to its high mechanical strength and favorable dust exclusion characteristics due to its tightly packed weave, as demonstrated in prior tumbler testing. Unlike the white appearance of Ortho and Teflon, Kevlar's natural yellow color may influence its optical performance. Additionally, a PTFE-laminated version of the JPS Kevlar® was included, which featured a solution coating of PTFE mixed with titanium dioxide (TiO_2) and a thin PTFE film laminate which was developed as part of a previous NASA led Small Business Innovative Research (SBIR) effort. This modified version was tested to evaluate whether the inclusion of TiO_2 in a coating could mask the optical properties of the underlying fabric substrate.

E. Equipment and Method Used for Optical Measurements in this Effort

A 410 Solar Reflectometer was used for the absorptance testing for this effort. It is a portable instrument which provides a fast, field-usable estimate of how well a surface reflects solar radiation across the solar spectrum. It uses a broadband light source and filtered detectors to simulate solar energy across four spectral bands (UV, visible, near-infrared (IR), and mid-IR) that collectively approximate the solar spectrum. These bands are weighted and combined to approximate total solar reflectance per standard solar irradiance curves (e.g., AM0-vacuum or AM1.5-atmosphere). It compares the reflected energy from the sample to that of a built-in reference standard to compute a solar reflectance as a percentage. To measure the fabric specimens, the reflectometer was set to a solar irradiance of AM0 (air mass = 0) to reflect conditions in the vacuum of space.

Figure 3. Ortho Panels Post Tumbler Dust Exposure. *(Top) Left half covered with dust simulant, right half brushed. (Bottom) Post vacuuming.*

A Devices & Services ET-100 Emissometer was used for emissivity testing[11]. It is a portable, precision emissometer designed to measure total normal emittance in accordance with ASTM E408. The device uses thermal comparison between the test sample and reference standards of known emittance. It heats the sample slightly above ambient using an internal heater. Infrared detectors measure the thermal radiation emitted from both the sample and reference surface. The system compares the signal from the test surface to calibrated standards (typically $\varepsilon \approx 0.05$ for polished metal and $\varepsilon \approx 0.90$ for matte black) and calculates the sample's emittance.

For this effort, solar absorptance and emissivity measurements were taken for each fabric in its "neat" beginning of life condition, post tumbler exposure after brushing condition, and post tumbler after vacuuming condition.

Per the ASTM standard, for each fabric panel measurements were taken in three locations and averaged. Initial measurements were conducted with the fabrics placed over a black backer with the assumption that all fabrics were opaque. After the tumbler exposure, the fabric panel was removed from the tumbler, brushed one time as shown in Figure 3, and measurements were taken. Finally, the fabric panel was then vacuumed, and three additional measurements were taken. The average values of the measurements were tabulated for comparison.

Later assessment determined that the assumption that every fabric panel was opaque could be incorrect. Therefore, to capture the effects of transmission, a second round of absorptance measurements were taken with the fabrics backed by MLI. In addition, the emissivity of Ortho Fabric was measured with an MLI backer.

III. Test Results

A. Absorptance Measurements

Three measurements of each panel of Ortho, Kevlar, Teflon T-162 and PTFE laminated Kevlar under various conditions were taken and the average values are shown in Table 3. Included are the computed transmittance and solar absorptance based on the calculations described in Section II, A. When assessing the variability between the individual measurements, the standard deviations range from 0.001 to 0.0179, with an average of approximately 0.0058, indicating good repeatability across all measurements. Most values fall below 0.01, reflecting tight agreement between replicates. Higher variability is observed in dust-contaminated conditions, likely due to non-uniform surface coverage. Overall, the variability is small relative to the observed changes in absorptivity, supporting confidence in the reported trends.

Table 3: Absorptance Measurements for Tested Fabrics Pre and Post Dust Exposure

	Pre Dust Exposure				Post Dust Exposure		
	Neat	Neat	Calculated Transmittance	Calculated Absorptance	Post Brushing	Post Vacuuming	Post Vacuuming
					NU-LHT-4M	NU-LHT-4M	CSM-LHT-1
	Black	MLI			Black	Black	Black
Ortho	0.200	0.119	0.107	0.106	0.452	0.362	0.371
Kevlar	0.345	0.296	0.122	0.262	0.471	0.437	-
Teflon	0.278	0.090	0.378	0.059	0.449	0.431	-
PTFE Kevlar	0.340	0.320	0.038	0.308	0.365	0.354	-

Figure 4 is a graphical representation of the data in Table 3.

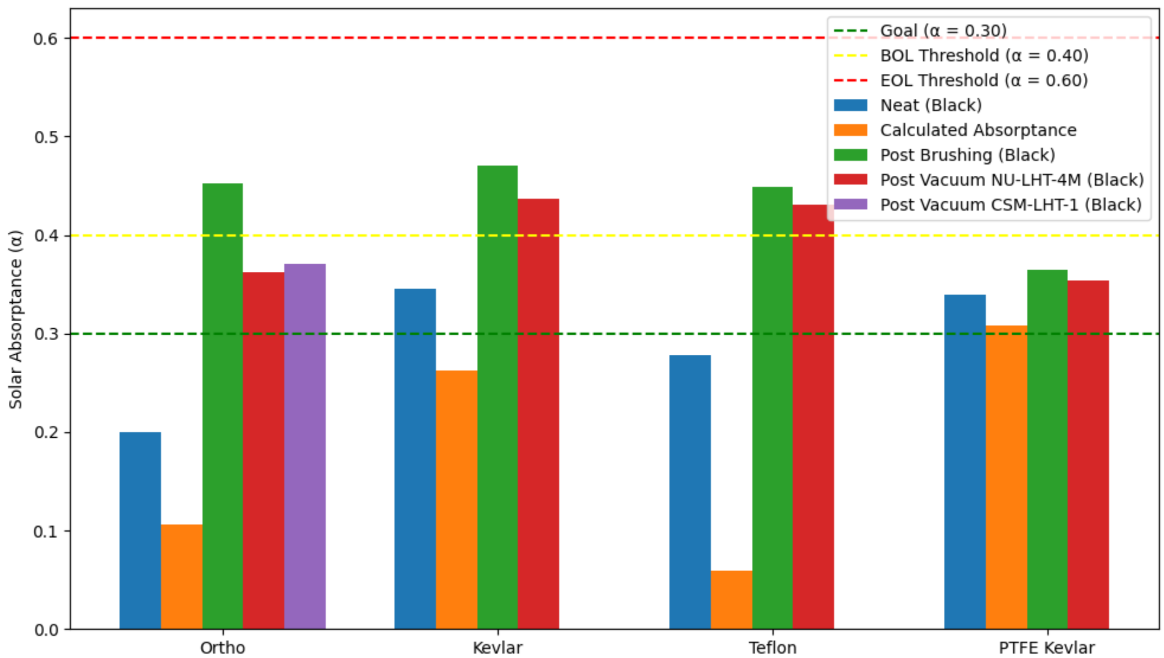

Figure 4. Absorptance Measurements for Tested Fabrics Pre and Post Dust Exposure

The absorptance measurements show clear material-dependent differences both before and after dust exposure. In the neat condition, Ortho and Teflon exhibit the lowest apparent absorptance values when measured over a reflective MLI backing, indicating higher transparency and greater sensitivity to backing effects. Kevlar and PTFE-Kevlar, by contrast, show higher neat absorptance values and smaller differences between black and MLI backings, consistent with more optically opaque constructions. All four fabrics meet the ASM clean absorptance threshold (<0.3) in the neat condition.

Following dust exposure, all fabrics exhibit increased absorptance, reflecting dust retention and surface darkening. Post-tumbler cleaning by vacuuming reduces absorptance relative to the brushed state but does not fully recover neat-condition values. Comparing post brushing to post vacuuming, vacuuming results in slightly lower absorptance than brushing, suggesting improved removal of embedded or fine particulate, although the magnitude of improvement varies by fabric. Ortho and Kevlar show similar post-cleaning absorptance values, while Teflon and PTFE-Kevlar retain somewhat lower values, indicating better resistance to dust-induced optical degradation.

A comparison between Kevlar and PTFE–Kevlar indicates that the addition of a PTFE film with TiO_2 significantly reduces dust-driven increases in solar absorptance and helps the composite fabric retain optical properties closer to its clean condition. While the neat absorptance values of Kevlar and PTFE–Kevlar are similar, the PTFE–Kevlar system exhibits substantially lower calculated transmittance, indicating that the film creates a more optically closed system that is less sensitive to underlying layers. Following dust exposure and subsequent cleaning, Kevlar shows a pronounced increase in absorptance, whereas PTFE–Kevlar demonstrates a much smaller rise and better recovery after both brushing and vacuuming. This behavior is consistent with the presence of the TiO_2-loaded PTFE film, which increases solar scattering and reflectance, limits dust embedding by providing a smoother and lower-surface-energy interface and reduces optical trapping within the fibrous Kevlar substrate[12]. As a result, PTFE–Kevlar maintains greater margin relative to ASM absorptance requirements in the dirty condition and trends closer to the clean-condition goal, displaying the effectiveness of the PTFE/TiO_2 film as an optical stabilization and dust-mitigation layer for lunar EPG applications.

Regarding the difference between simulants, after vacuum cleaning Ortho Fabric exhibits very similar absorptance values for both simulants, with NU-LHT-4M measuring 0.362 and CSM-LHT-1 measuring 0.371 on a black backing. The slightly higher absorptance observed with CSM-LHT-1, corresponding to an increase of approximately 0.009 absorptance units (~2.5%), suggests marginally greater residual dust retention or surface darkening relative to NU-LHT-4M under identical cleaning conditions. This behavior may be attributable to differences in particle size distribution, morphology, or adhesion characteristics between the simulants, which can influence how effectively fine particulates are removed from the Ortho weave during vacuuming. While the difference is small and both values remain well below the ASM dirty-condition absorptance threshold, the trend indicates that CSM-LHT-1 produces a slightly more persistent optical impact on Ortho compared to NU-LHT-4M after vacuum cleaning.

When transmittance is accounted for, the calculated absorptance values highlight the role of fabric transparency. Ortho and Teflon exhibit the highest calculated transmittance, confirming that a significant fraction of incident solar energy is transmitted rather than absorbed by the fabric itself. As a result, their apparent absorptance measured with a black backing overestimates true material absorption. Kevlar and PTFE-Kevlar show much lower transmittance, behaving more like opaque materials, and therefore their calculated absorptance values more closely reflect intrinsic surface behavior.

In relation to ASM project requirements, all four fabrics meet the dirty-condition absorptance threshold (<0.6) after dust exposure and cleaning. However, Ortho and Teflon approach the clean-condition goal only after accounting for transmittance, underscoring the importance of backing selection and full system context when evaluating partially translucent outer shell fabrics. Overall, the results demonstrate that both material construction and optical transparency strongly influence measured absorptance, and that comparative post-dust performance must be interpreted in conjunction with cleaning effectiveness and representative EPG layup conditions.

B. Emissivity Measurements

The average emissivity values measured for various conditions of Ortho, Kevlar, Teflon T-162 and PTFE laminated Kevlar fabrics are shown in Table 4.

Table 4: Emissivity Measurement for Tested Fabrics Pre and Post Dust Exposure

	Pre-Tumbler		Post-Tumbler		
	Neat	Neat	Post Brushing	Post Vacuuming	Post Vacuuming
			NU-LHT-4M	NU-LHT-4M	CSM-LHT-1
	Black	MLI	Black	Black	Black
Ortho	0.837	0.826	0.860	0.866	0.870
Kevlar	0.817	-	0.857	0.840	-
Teflon	0.836	-	0.831	0.867	-
PTFE Kevlar	0.879		0.876	0.892	-

Figure 5 is a graphical representation of the data in Table 4.

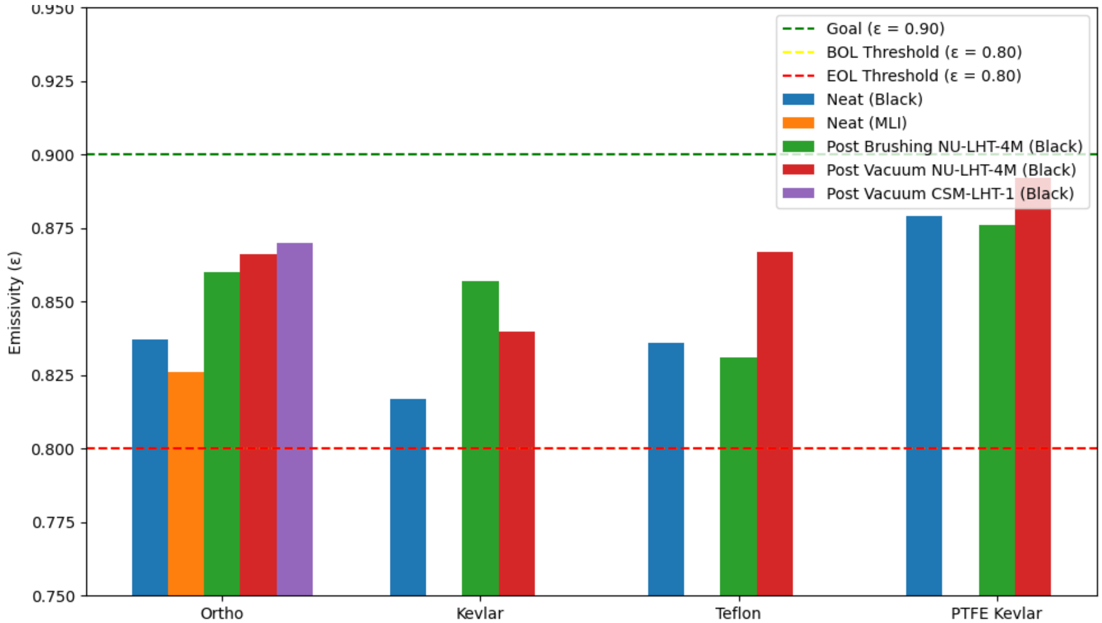

Figure 5. Emissivity Measurements for Tested Fabrics Pre and Post Dust Exposure

The emissivity data show relatively small variation across fabrics and exposure conditions, with all materials maintaining high emissivity values both before and after dust exposure. In the neat condition, Ortho, Kevlar, and Teflon cluster in a narrow range between approximately 0.82 and 0.84, while PTFE–Kevlar exhibits the highest baseline emissivity at approximately 0.88, indicating a more intrinsically emissive surface. These differences suggest that fabric construction and surface finish influence emissivity to a lesser degree than absorptance, with all candidates already performing near or above the ASM BOL and EOL thresholds in the clean state.

The Ortho emissivity measurements show a small but consistent difference between black and MLI backings in the neat condition, with the black backing yielding a slightly higher emissivity (~0.837) than the MLI backing (~0.826). This behavior indicates that Ortho is not fully opaque in the infrared and that the measured emissivity is influenced by the optical properties of the backing material. The lower value measured over the reflective MLI backing reflects partial transmission of thermal radiation through the fabric and subsequent reflection back into the sensor, effectively reducing the apparent emissivity attributed solely to the Ortho surface. This sensitivity to backing confirms that Ortho behaves as a partially translucent material and reinforces the importance of representative backing selection when interpreting emissivity data albeit to a lesser extent than absorptance. In the context of the EPG system, where Ortho would be backed by reflective MLI layers, the MLI-backed measurement is more representative of in-service performance, while the black-backed measurement provides a conservative, bounding case.

Dust exposure produces a modest but generally positive increase in emissivity for most fabrics, particularly after brushing and vacuum cleaning. This trend is consistent with dust particles increasing surface roughness and effective radiating area, which can enhance thermal emission[13]. The magnitude of change, however, is limited, typically on the order of 0.02–0.04, indicating that emissivity is comparatively insensitive to dust relative to solar absorptance. Vacuum cleaning tends to yield equal or slightly higher emissivity values than brushing, suggesting that while fine particulate may remain after cleaning, the overall surface condition remains favorable for thermal radiation.

Comparing Kevlar to PTFE–Kevlar, the presence of the PTFE film with TiO_2 appears to provide a measurable benefit in emissivity stability and absolute performance. PTFE–Kevlar not only starts with a higher neat emissivity than bare Kevlar but also shows a higher final value after dust exposure and cleaning, reaching almost to the ASM emissivity goal. The TiO_2-loaded PTFE film likely contributes through its inherently high infrared emissivity and by providing a more uniform surface that maintains radiative efficiency even after dust interaction. In contrast, bare Kevlar, while still meeting requirements, exhibits lower absolute emissivity and smaller post-exposure gains.

Overall, all tested fabrics remain well above the ASM emissivity BOL and EOL threshold value of 0.8, demonstrating strong margin with respect to minimum requirements. Several cases, most notably PTFE–Kevlar after dust exposure and vacuum cleaning, approach or exceed the ASM goal value of 0.9. These results indicate that emissivity is not a limiting parameter for the candidate fabrics and that surface treatments such as a TiO_2-loaded PTFE film can further enhance thermal performance while maintaining robustness to dust exposure and cleaning.

C. Previous Optical Measurements of Fabrics Exposed to Low Earth Orbit

The optical properties of Ortho and Kevlar fabrics were previously tested and detailed in NASA/TM-2017-219634 "Comparison of High-Performance Fiber Materials Properties in Simulated and Actual Space Environments." This report summarizes testing on a variety of fabrics for durability in Low Earth Orbit (LEO) as a part of the Materials Internation Space Station Experiment (MISSE)[14]. Among the properties tested, solar absorptance and infrared emittance were measured on the fabrics both before and after exposure. A control sample and flown sample of both fabric's measured values are listed in Table 5.

Table 5: Previous Optical Property Measurement for Ortho and Kevlar

Sample	Solar Absorptance		% Change	Solar Emittance		% Change
	Preflight	Postflight		Preflight	Postflight	
Ortho (not flown)	0.308	0.332	+7.79%	0.85	0.86	+1.18%
Ortho (flown - ram)	0.347	0.425	+22.48%	0.85	0.86	+1.18%
Kevlar (flown - wake)	0.413	0.445	+7.75%	0.83	0.83	0%
Kevlar (flown - ram)	0.416	0.432	+3.85%	0.84	0.86	+2.38%

Samples mounted on the ram side directly face the direction of orbital motion, experiencing maximum atomic oxygen (AO) flux as residual atmospheric oxygen atoms impact the surface at orbital velocity, along with continuous solar ultraviolet (UV) exposure. This environment accelerates oxidative erosion and surface chemistry changes, which drive increases in solar absorptance. By contrast, wake-side samples are partially shielded from AO by the station structure and orbital flow shadowing, receiving significantly lower AO exposure while still experiencing UV radiation.

A comparison of the absorptance values obtained in the 2017 study (Ortho~0.31; Kevlar~0.41) to those acquired in this effort (Ortho~0.2; Kevlar~0.35) do not perfectly align and thus left the ASM team with questions regarding the accuracy of both sets of data. However, several key differences potentially explain the discrepancies.

First, the 2017 report states that Solar absorptance was measured with an AZ Technology Laboratory Portable Spectroreflectometer-300 (LPSR-300) versus the 410 Solar Reflectometer used for this effort. The two devices differ in their spectral response ranges. The LPSR 300 integrates over a broader range and an additional portion of the solar spectrum extending further into the near-infrared where fabrics can absorb or transmit more energy, leading to a higher reported absorptance. The LPSR 300 takes many reflectance measurements from wavelengths of 250 to 2800 nm.

Comparatively, the 410 Solar Reflectometer used in this test only takes 14 reflectance measurements in 7 wavelength bands: 335 to 380 nm, 400 to 540 nm, 480 to 600 nm, 590 to 720 nm, 700 to 1100 nm, 1000 to 1700 nm, and 1700 to 2500 nm. The 410 Solar Reflectometer takes the sum of reflectance measurements at the 7 wavelengths bands, whereas the LPSR 300 used in the 2017 study takes the sum of all reflectance measurements at approximately 100 various wavelengths. The reflectance measurements from the wavelength of 1700 to 2500 nm account for 1/7th of the 410 Solar Reflectometer's measurements. The same wavelength range accounts for roughly 25% of the LPSR 300 reflectance measurements. The addition of the lower reflectance values in the 1700 to 2500 nm wavelength range can explain the difference of absorptivity measurements between instruments.

Second, measurement geometry may play a role. The LPSR 300 employs a hemisphere lens, while the 410 Reflectometer uses a fixed-angle (60°) setup, which may influence how the instrument captures scattered vs. specular reflections from the textured fabric surface. Differences in how the instruments contact the sample and compensate for surface irregularities or gaps between the fabric and the backing could also affect results, with the LPSR potentially allowing more backscatter or leakage that would artificially lower reflectance and increase apparent absorptance.

Furthermore, while both tests used a black backing, Ortho is partially transmissive in some parts of the solar spectrum as evidenced by the differing measurements taken with the MLI backer. If the LPSR setup allowed transmitted light to reflect off the backing and be partially absorbed, this could further inflate absorptance. In contrast, the 410 Reflectometer may be more sensitive to reflectance and less influenced by transmitted losses, especially if designed for use on opaque materials.

Finally, different fabric samples, possibly with different surface conditions, were used in the tests. Minor differences such as fiber abrasion, yellowing, or embedded dust could also contribute to variations in optical performance. Taken together, these factors suggest that the lower absorptance reported by the 410 Reflectometer is likely due to differences in spectral weighting, geometry, and measurement sensitivity to transmittance and fabric texture.

The LPSR 300 is more accurate in a laboratory setting for precise spectral characterization and its output is better suited for preparing inputs for thermal and optical simulation tools. The 410 is more application oriented, providing values directly relevant to solar exposure scenarios. It provides quick, practical value for solar absorptance for materials in a known configuration (i.e. when the backer material is known).

The differences in emissivity values between the 2017 study (Ortho~0.85; Kevlar ~0.83) and this one (Ortho~0.83; Kevlar~0.82) are less pronounced. The historical values were obtained using the AZ Technology TEMP-2000A infrared reflectometer, while the current measurements were taken using the ET-100 emissometer. These modest reductions in measured emissivity are likely to be due to differences in the instruments' optical geometries, spectral response ranges, and surface interaction methods. The TEMP-2000A and ET-100 may respond differently to textured or semi-transmissive fabric surfaces, especially given that both Ortho and Kevlar can exhibit some degree of microstructural variability. Additionally, calibration differences and detector sensitivity across thermal IR bands (typically 3–35 µm) may contribute to small but consistent deviations. It's also possible that surface condition, handling, or slight aging of the fabric between tests could have contributed to reduced emissivity in the current data. Despite these differences, the values remain broadly consistent.

D. Additional Emissivity Measurements

In addition to the aforementioned fabrics, the ASM team conducted emissivity measurements on additional candidate fabrics of interest outside of this effort. They are included in Table 6 for reference to aid in the emissivity characterization of various fiber types. All measurements were taken with a black backing fabric using the ET-100 emissometer.

Table 6: Emissivity Measurement for Additional Fabrics Pre and Post Dust Exposure

Fabric	Fiber Type	Emissivity Measurements (ε)	
		Neat	Post Dust Vacuumed
Warwick Turtleskin T9-816a	Vectran	0.870	0.883
Warwick Turtleskin T9-1410a	Vectran	0.848	-
Insulsafe Textiles Twaron w SS	Twaron	0.831	-
Kozane Pyro 500.2009	Kevlar	0.825	0.845
Dupont Kevlar EXO CM E1100H	Kevlar	0.739	-
Dupont Kevlar EXO FA E150H	Kevlar	0.737	-
Newtex F-500	Fiberglass	0.732	-
Albarrie Needlepunch	P84	0.683	0.839

The emissivity data for the additional fabrics shows a potential trend as a function of fiber type, with high-performance organic fibers generally exhibiting higher emissivity than inorganic or glass-based constructions. Among the Vectran-based fabrics, both Warwick Turtleskin variants exhibit relatively high neat emissivity, with T9-816a measuring approximately 0.87 and T9-1410a slightly lower at approximately 0.85. These values indicate strong intrinsic radiative capability and are consistent with tightly woven, high-mass organic fibers that present a continuous radiating surface. The Twaron SS fabric shows slightly lower emissivity (~0.83) but remains well above typical minimum thermal requirements and comparable to other aramid-based textiles.

Within the Kevlar family, emissivity spans a broader range depending on construction and finishing. Kozane Pyro 500.2009 exhibits moderate neat emissivity (~0.83), while the DuPont Kevlar EXO CM E1100H and FA E150H fabrics show noticeably lower values (~0.74). This spread suggests that weave architecture, surface finish, and possible yarn treatments play a significant role in determining emissivity beyond fiber chemistry alone. The fiberglass fabric (Newtex F-500) exhibits a similarly low emissivity (~0.73), consistent with smoother, more reflective inorganic fibers that are less efficient infrared emitters. The P84 Albarrie needle-punched fabric shows the lowest neat emissivity (~0.68), reflecting its fiber chemistry and lofted structure, which may reduce effective radiating surface area in the infrared.

Where post-dust vacuumed data are available, emissivity increases relative to the neat condition. Kozane Pyro 500.2009 increases from approximately 0.83 to 0.85, Warwick Turtleskin T9-816a increases from approximately 0.87 to 0.88, and Albarrie needle-punch shows a pronounced increase from approximately 0.68 to 0.84. These increases are consistent with dust deposition increasing surface roughness and effective emissive area, even after vacuum cleaning. The particularly large increase observed for the P84 needle-punched fabric suggests that its open, porous structure retains fine particulate that substantially alters its radiative behavior. Overall, the data indicate that while intrinsic emissivity is strongly influenced by fiber type, dust exposure and residual particulate can significantly elevate emissivity, particularly for low-baseline or highly porous fabrics, and that vacuum cleaning does not necessarily return emissivity to neat-condition values.

IV. Conclusion

The Artemis Suit Materials Team conducted absorptance and emissivity testing on candidate outer shell fabrics to assess compliance with current optical property requirements using Ortho Fabric as the baseline reference. Baseline measurements were established for both clean beginning-of-life conditions and degraded end-of-life states. EOL conditions were simulated using a rotary tumbler abrasion stressor incorporating lunar dust simulant and ceramic media to reproduce the cumulative mechanical wear and contamination expected during extended lunar surface operations. This approach enabled a consistent evaluation of fabric optical performance across realistic mission-relevant conditions.

Solar optical properties were measured using a combination of ASTM C1549 portable reflectometer methods and ASTM E903 laboratory-based principles. The effects of backing material were explicitly examined to understand how partial fabric transparency influences measured values and to better represent the EPG system configuration. Absorptance measurements revealed clear material-dependent differences in both neat and dust-exposed states. Following dust exposure, all fabrics exhibited increased absorptance, consistent with dust retention and surface darkening. Post-tumbler cleaning by vacuuming reduced absorptance relative to the brushed condition but did not fully restore neat-condition values, indicating persistent optical impact from embedded fine particulates.

The results further demonstrate that the addition of a PTFE film with TiO_2 provides a measurable benefit by significantly reducing dust-driven increases in solar absorptance and helping composite fabrics retain optical properties closer to their clean state. Calculated absorptance values, which account for transmittance effects, highlighted the important role of fabric transparency, particularly for lighter or more porous constructions, and reinforced the need to interpret black-backed measurements conservatively for partially translucent materials.

In contrast to absorptance, emissivity showed relatively small variation across fabrics and exposure conditions. All materials maintained high emissivity values in both neat and dust-exposed states, remaining above BOL and EOL threshold requirements. Dust exposure generally produced a modest increase in emissivity, particularly after brushing and vacuum cleaning, consistent with increased surface roughness and effective radiating area. Emissivity was therefore not identified as a limiting parameter for any of the candidate fabrics evaluated.

Concerning the use of different simulants, measured results indicate that both produced a significant increase in solar absorptivity; however, differences in magnitude suggest that simulant-specific properties—such as particle size distribution, morphology, and mineral composition—affect dust retention and optical response. NU-LHT-4M generally resulted in slightly higher absorptivity increases compared to CSM-LHT-1, indicating a potentially greater tendency for surface adherence or light absorption.

These findings are relevant to lunar missions, as actual lunar regolith exhibits a wide range of particle sizes, angularity, and optical characteristics depending on location and maturity. As a result, the choice of simulant can influence predicted degradation in thermal control performance. This highlights the importance of considering multiple simulants when evaluating material performance to better bound on-orbit behavior and reduce uncertainty in EPG design.

While the use of portable instruments such as the Devices & Services 410 Solar Reflectometer and the ET-100 emissometer enabled efficient, repeatable comparison across a large test matrix, these methods are inherently less accurate than full laboratory-based spectral techniques. As such, measured values may vary depending on instrument calibration, test setup, and backing material selection. The results underscore the importance of clearly defining backing conditions and recognizing the comparative nature of portable measurements when interpreting fabric optical performance. Overall, the testing demonstrates that several candidate fabrics meet current ASM optical property requirements with margin, while surface treatments such as PTFE/TiO_2 films offer meaningful advantages for maintaining optical performance under lunar dust exposure.

Due to the sensitivity of the optical measurement instruments, this study was limited to evaluating fabrics after cleaning and was not able to directly characterize the optical properties of dust-laden surfaces. However, during lunar operations, dust accumulation will persist throughout an EVA and cleaning will typically occur only at its conclusion. Future testing should therefore prioritize measurement of fabrics in their as-contaminated state to better represent in-situ thermal performance.

Additionally, dust exposure in this study was limited to an 8-hour rotary tumbler condition. While this provides a useful baseline, further work is needed to correlate tumbler duration with actual EVA exposure time and dust loading. Several materials approached threshold absorptivity limits under the conditions tested, suggesting that longer-duration exposure may further degrade optical performance. This has direct implications for maintaining thermal equilibrium in the suit and may necessitate considerations such as reduced EVA duration or enhanced thermal management strategies.

It is also important to note that lunar regolith properties vary significantly with location and maturity. Permanently shadowed regions (PSRs), particularly at the lunar south pole, may contain darker and more optically absorptive material than that encountered during the Apollo missions, while also existing in substantially colder thermal environments. These factors introduce additional uncertainty and potential risk in extrapolating current results to future mission conditions.

Finally, future efforts should investigate dust-resistant coatings and surface treatments aimed at reducing dust adhesion and retention. The methodologies established in this study provide a foundation for quantitatively assessing such technologies and their effectiveness in preserving optical performance under lunar-relevant conditions.

Acknowledgments

This document was created with assistance from Microsoft Co-pilot for interpretation of results and editing text. The content has been reviewed and edited by Robert Jones.

References

[1] M. Winter and D. Duda, Thermal Optical Properties Characterization of Space Suit Materials, NASA Technical Memorandum NASA/TM–2018–219423, NASA Johnson Space Center, 2018. [Online]. Available: https://ntrs.nasa.gov/api/citations/20180003390/downloads/20180003390.pdf

[2] ASTM International, *ASTM C1549-16(2023), Standard Test Method for Determination of Solar Reflectance Near Ambient Temperature Using a Portable Solar Reflectometer*, ASTM International, West Conshohocken, PA, USA, 2023.

[3] ASTM International, *ASTM E903-20, Standard Test Method for Solar Absorptance, Reflectance, and Transmittance of Materials Using Integrating Spheres*, ASTM International, West Conshohocken, PA, USA, 2020.

[4] *410-Solar Handheld Reflectometer Product Data Sheet*, Surface Optics, San Diego, CA., 2021. Accessed 26 March 2025.

[5] M. Winter, J. Campbell, and B. Grauman, *Evaluation of Optical Property Measurement Methods for Space Suit Materials*, NASA Technical Publication NASA/TP-2019-220552, NASA Johnson Space Center, Houston, TX, 2019.

[6] S. Kapur, "Radiation Basics: Making Sense of Emissivity & Absorptivity," *Electronics Cooling*, Mar. 2025. [Online]. Available: https://www.electronics-cooling.com/2025/03/radiation-basics-making-sense-of-emissivity-absorptivity/

[7] ASTM International, *ASTM E408-13(2021), Standard Test Methods for Total Normal Emittance of Surfaces Using Inspection-Meter Techniques*, ASTM International, West Conshohocken, PA, USA, 2021.

[8] C. Peabody, "Rotary Tumbler Abrasion Test Procedures," National Aeronautics and Space Administration, CTSD-ADV-2143, 26 February 2024.

[9] R. J. Jones, S. Wilson, T. Brady, D. Morris, R. Rhodes, S. McFarland, B. Conger, and N. Anderson, "Establishing Standardized Test Methods for Evaluating Space Suit Gloves," in *Proc. International Conference on Environmental Systems (ICES)*, 53rd ICES, 2023, Paper ICES-2023-37.

[10] R. J. Jones, "Validation Testing and Statistical Analysis of the Rotary Tumbler Fabric Abrasion Method," in *Proc. International Conference on Environmental Systems (ICES)*, 54th ICES, 2024, Paper ICES-2024-50.

[11] Devices & Services ET-100 Emissometer https://www.devicesandservices.com/AE1%20Spec%20Sheet.pdf

[12] M. Ali, S. Basu, and A. Sinha, "Dust transport and adhesion on lunar surface: A review of mechanisms, modeling and mitigation strategies," *Materials Chemistry and Physics*, vol. 317, p. 128739, 2024. [Online]. Available: https://doi.org/10.1016/j.matchemphys.2024.128739

[13] J. R. Gaier, "The effects of lunar dust on EVA systems during the Apollo missions," *NASA/TM-2005-213610*, NASA Glenn Research Center, Cleveland, OH, USA, 2005.

[14] M.M. Finckenor, "Comparison of high-performance fiber materials properties in simulated and actual space environments," National Aeronautics and Space Administration, NASA/TM-2017-219634, 1 July 2017. [Online]. Available: https://ntrs.nasa.gov/citations/20170006996